4
Application to the TA-40 Manipulator

4.1.
Introduction

Until now only the theoretical principles used in this thesis have been covered. This chapter covers how this theory is applied to the TA-40 manipulator.

The TA-40 is a robotic manipulator used by PETROBRAS in underwater interventions. It is attached to a ROV (Remote Operating Vehicle) that will take it to its working environment at great depths off-shore. The manipulator is currently controlled by tele-operation and it does not offer the repeatability nor absolute precision required to perform more refined automated task.

First, a brief description of the manipulator will be given, and then a more thorough description of every link and joint that constitutes the manipulator. The nominal measurements of the TA-40 will be implemented in the Denavit-Hartenberg notation to estimate the kinematics of the manipulator.

4.2.
Description of the Manipulator

The TA-40 is a hydraulic manipulator capable of lifting 210kg at the maximum reach of 1950mm. It has 6 rotational joints, resulting in 6 degrees of freedom. At the end-effector a gripper is attached.

It has been created to operate in hostile environments and it is capable of working at sea depths of 3000 meters.

At present it is operated by a master-slave configuration, where the master is represented by a miniature manipulator, shown in Figure 33.

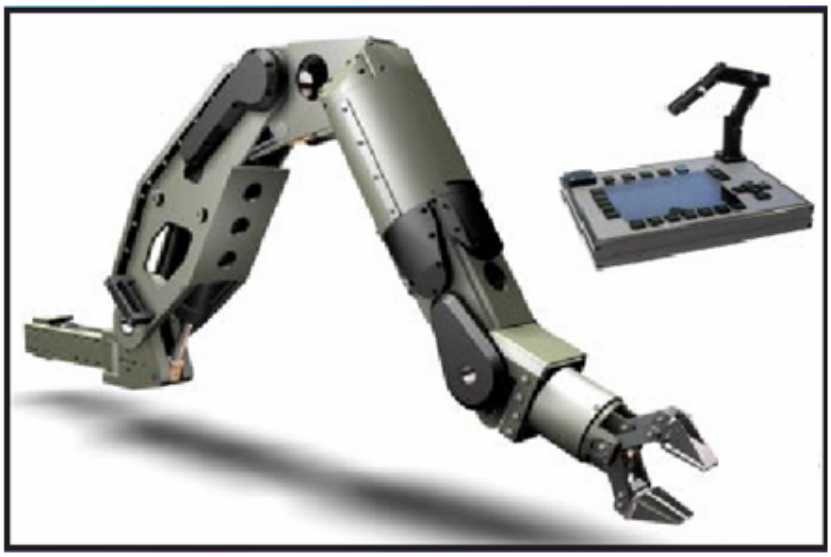

Figure 33 – TA40 and the miniature robot used as master

With the increased precision and repeatability attained by calibration, the trajectories of the robot can be developed "offline" in a virtual environment, reducing the time and cost of the process.

4.3. Kinematics of the TA-40

A kinematic model of the manipulator is necessary to perform the calibration of the manipulator structure. The theoretical part is deduced in Chapter 2. Figure 34 shows the manipulator and the 7 frames (coordinate systems), one at each joint and one at the end effector. The following sections show how the Denavit-Hartenberg parameters of the TA-40 are obtained.

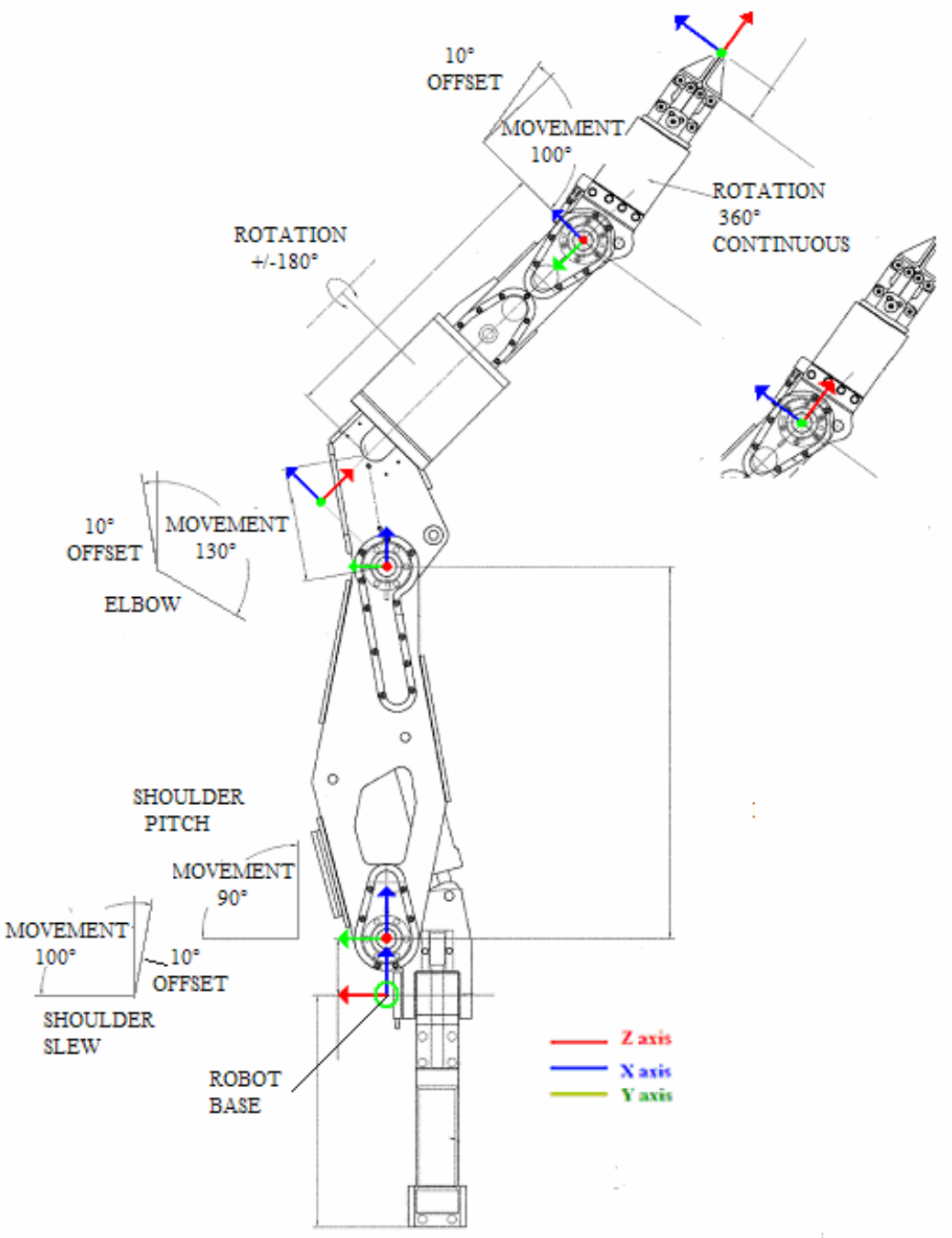

Figure 34 – TA-40 and coordinate systems [1]

4.3.1.
Joints 1 and 2

The center of joint 1 (O_0) is situated at the manipulator base. The axis z_0 represents the rotation axis of joint 1. The axis x_0 is the common normal between the frame centers O_0 of joint 1 and O_1 of joint 2. The fixed distance between the centers O_0 and O_1 along the common normal is 115 mm and it is represented by a_1=115 in the DH-notation. Looking in the direction of x_0, the z_1 axis is rotated 90º relative to the z_0 axis. This angle is represented by α_1=90º. The distance between the frame centers in direction z_0 is zero, and it is represented by d_1=0.

4.3.2.
Joints 2 and 3

The distance between the frame centers, O_1 and O_2, along the common normal is 753mm giving a_2=753. The rotation axes, z_1 and z_2, are parallel, giving α_2=0º. The distance between O_1 and O_2 along z_1 is zero, giving d_2=0.

4.3.3.
Joints 3 and 4

The distance between the frame centers is 188 mm giving a_3=188. The position of O_3 is outside the structure of the manipulator. The axis z_3 is rotated 90º around the x_2 axis, giving α_3=90º. The distance between the respective frame centers along z_2 is zero, giving d_3=0.

4.3.4.
Joints 4 and 5

The frame center O_4 of joint 5 is located 747mm along the z_4 axis from O_4, giving d_4=747. Since the frame centers position along the common normal is zero, a_4=0. The z_4 axis is rotated -90º relative to z_3, giving α_4=-90º.

4.3.5.
Joints 5 and 6

The frame centers, O_4 and O_5, are situated at the same position, giving d_5=0, a_5=0. The z_5 axis is rotated 90º relative to the z_4 axis, giving α_5=90º.

4.3.6.
Joint 6

O_6 is situated 360mm along the z_5 axis. This gives d_6=360 and a_6=0. Since there is no joint located at O_6, the orientation of frame 6 can be chosen arbitrarily as long as x_5 and x_6 are parallel when θ_6=0°. The z_6 axis is chosen so that it coincides with the z_5 axis. There is no rotation along the common normal giving α_6=0º.

4.3.7.
Denavit-Hartenberg Parameters

Table 1 contains all the Denavit-Hartenberg parameters. From these the parameters transformation matrices, *Ai*, can be given to calculate the kinematics of the manipulator using Eqs. (6) and (8).

Link i	a_i [mm]	d_i [mm]	α_i [º]	θ_i
1	115	0	90	θ_1
2	753	0	0	θ_2
3	188	0	90	θ_3
4	0	747	-90	θ_4
5	0	0	90	θ_5
6	0	360	0	θ_6

Table 1 – Denavit-Hartenberg parameters

4.4. Calibration of the TA-40

This chapter explains how the theory in chapter 2.4 is applied to the TA-40 manipulator.

In order to estimate the generalized errors, all the redundant errors have to be eliminated. This is done by transferring the values of the redundant errors using Eq. (21) for i=1:6. The redundant errors $\varepsilon_{z,(i)}$ and $\varepsilon_{r,(i)}$ could then be eliminated for i=0:5. The error $\varepsilon_{z,(6)}$ cannot be eliminated since its contribution to the end-effector position is not passed on to another joint. The errors $\varepsilon_{p,6}$ $\varepsilon_{s,6}$, and $\varepsilon_{r,6}$ can be eliminated since they are rotational errors and do not effect the end-effector position. This eliminates 15 errors in total. Further, there exists another relation between the redundant errors given in Eq.(27). Rearranging this equation gives:

$$\begin{cases} \varepsilon^{*}_{x,(5)} = \varepsilon_{x,(5)} + \varepsilon_{s,(5)} \cdot \mathrm{d}_6 \\ \varepsilon^{*}_{p,(5)} = \varepsilon_{p,(5)} - \dfrac{\varepsilon_{y,(5)}}{\mathrm{d}_6} \end{cases} \tag{167}$$

This means that $\varepsilon_{s,5}$, and $\varepsilon_{y,5}$ can be eliminated from the model, leaving only 25 errors to estimate. The reduced identification jacobian (G_e) has only 25 elements. The matrix $G_e^T G_e$ is then invertible. Substituting J_t with G_e in Eq.(14) gives a solution to the equation.

Eliminating $\varepsilon_{s,5}$ and associating it with the translational error means that the orientation error of the end-effector cannot be estimated independently. Neither can the orientation of link 5. However, the estimated orientation of link 5 will have a fixed bias to the true orientation for all configurations of the joints. This means that a camera on link 5 will be able to detect the pose differences between two views.

4.5. Inverse Kinematics

The inverse kinematics in this chapter was deducted in [24]. It is presented in this thesis due to the importance for automation purposes.

It is impossible to develop a general method to estimate the inverse kinematics for a manipulator. Therefore the steps developed in this chapter cannot be applied directly to another manipulator. Using the specific properties of the TA-40 makes it possible to find a solution. The 5 joints 2, 3, 4, 5 and 6 are all situated within a plane in 3D space. Their respective frames (coordinate systems) are O_1, O_2, O_3, O_4 and O_5. A graphic interpretation of this plane is given in Figure 35.

Equation (168) gives the position and orientation of the end-effector in base coordinates.

$$T_6^0(\theta) = A_1^0 A_2^1 A_3^2 A_4^3 A_5^4 A_6^5 \tag{168}$$

Equation (168) can be elaborated to give the coordinates of frame 5, P_5^1, relative to frame 1:

$$P_5^1 = P_4^1 = \left(A_1^0\right)^{-1} T_6^0 \left(A_6^5\right)^{-1} = A_2^1 A_3^2 A_4^3 A_5^4 \tag{169}$$

Equation (162) gives the relative position and orientation of frame 5 relative to frame 1. The frames *4* and *5* have the same position, meaning that the angle of joint 4 does not affect the position of frame 5. By interpretation of Figure 35 the following equations are obtained:

$$A_2^1 A_3^2 A_4^3 A_5^4 = P_5^1 = \begin{bmatrix} & a_2c_2 + a_3c_{23} + d_4s_{23} \\ R & a_2s_2 + a_ss_{23} + d_4c_{23} \\ & 0 \\ 0 & 1 \end{bmatrix} \tag{170}$$

$$\left(A_1^0\right)^{-1} P_5^1 \left(A_6^5\right)^{-1} = \begin{bmatrix} & (x - b_1a_6)c_1 + (y - b_2a_6)s_1 - a_1 \\ R & z - b_3a_6 \\ & (x - b_1a_6)s_1 - (y - b_2a_6)c_1 \\ 0 & 1 \end{bmatrix} \tag{171}$$

$$P_5^1 = P_4^1 = \begin{bmatrix} a_2c_2 + a_3c_{23} + d_4s_{23} \\ a_2s_2 + a_ss_{23} + d_4c_{23} \\ 0 \end{bmatrix} = \begin{bmatrix} (x - b_1a_6)c_1 + (y - b_2a_6)s_1 - a_1 \\ z - b_3a_6 \\ (x - b_1a_6)s_1 - (y - b_2a_6)c_1 \end{bmatrix} = \begin{pmatrix} x' \\ y' \\ z' \end{pmatrix} \quad (172)$$

From the third line in Eq.(172) the angle of the first joint is obtained:

$$\theta_1 = \tan^{-1}\left(\frac{y - b_2a_6}{z - b_1a_6}\right) + k\pi \quad (173)$$

Using the first two lines of Eq.(172) gives:

$$\begin{pmatrix} a_2c_2 + a_3c_{23} + d_4s_{23} \\ a_2s_2 + a_ss_{23} + d_4c_{23} \end{pmatrix} = \begin{pmatrix} x' \\ y' \end{pmatrix} \quad (174)$$

The movement between frame 1 and frame 4 can be interpreted as a manipulator with 2 degrees of freedom, since the distance (k) between O_2 and O_4 is constant.

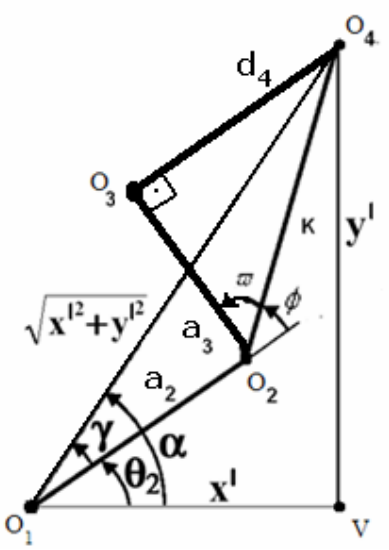

Figure 35 - A 2D interpretation of the frames O_2, O_3 and O_4. Frame O_5 coincides with frame O_4 [24].

From Eq.(174) and the 2D interpretation of the geometry in Figure 35 the following equations are obtained:

$$\begin{aligned} & k = \sqrt{a_3^{\,2} + d_4^{\,2}} \\ & a_2c_2 + k.\frac{a_3}{k}c_{23} + k.\frac{d_4}{k}s_{23} = a_2c_2 + k\cos(\theta_2 + \varpi) = x' \\ & a_2s_2 + k.\frac{a_s}{k}s_{23} + k.\frac{d_4}{k}c_{23} = a_2s_2 + k.\sin(\theta_2 + \varpi) = y' \\ & \varpi = \theta_3 - \phi \end{aligned} \quad (175)$$

Solving the equations for θ_2 and θ_3 gives:

$$\theta_2 = \tan^{-1}\left(\frac{y'}{x'}\right) + \cos^{-1}\left(\frac{x'^2 + y'^2 + a_2^2 - k^2}{2a_2\sqrt{x'^2 + y'^2}}\right) + \phi \qquad (176)$$

$$\theta_3 = -\cos^{-1}\left(\frac{x'^2 + y'^2 - a_2{}^2 - k^2}{2a_2 k}\right) + \tan^{-1}\left(\frac{d_4}{a_3'}\right) \qquad (177)$$

Having the angles of the first three joints and the desired position of the end-effector, it is possible to estimate the required angles of joints *4* and *5*. The movement of joint 6 does not change the position of the end-effector, only the orientation. The movement between frame *3* and the end-effector is given by Eq.(178).

$$A_4^3 A_5^4 A_6^5 = P_6^3 = \begin{bmatrix} & & d_6 c_4 s_5 \\ & R & d_6 s_5 s_4 \\ & & d_4 + d_6 c_5 \\ 0 & & 1 \end{bmatrix} \qquad (178)$$

$$P_6^3 = \left(A_3^0\right)^{-1} T = \left(A_1^0 A_2^1 A_3^2\right)^{-1} \cdot \begin{bmatrix} x \\ y \\ z \\ 1 \end{bmatrix} = \begin{pmatrix} x'' \\ y'' \\ z'' \\ 1 \end{pmatrix} \qquad (179)$$

$$\left(A_3^0\right)^{-1} T = \begin{bmatrix} & & -a_3 - a_2 c_3 + z s_{23} + y s_1 c_{23} + x c_1 c_{23} - a_1 c_{23} \\ & R & x s_1 - y c_1 \\ & & -z c_{23} + y s_1 s_{23} - a_2 s_3 + x c_1 s_{23} - a_1 s_{23} \\ 0 & & 1 \end{bmatrix} \qquad (180)$$

$$P_6^3 = \begin{bmatrix} a_1(c_{23}+s_{23}) + x c_1(c_{23}-s_{23}) + y s_1(c_{23}-s_{23}) + z(s_3 c_2 + c_3 s_2) - c_3 a_2 - a_3 \\ x s_1 - y c_1 \\ -a_1(s_2 c_3 + c_2 s_3) + z(s_{23} - c_{23}) + x(s_3 c_{12} + c_{13} s_2) + y(s_{13} c_2 + c_3 s_{12}) - s_3 a_2 \end{bmatrix}$$
$$= \begin{pmatrix} x'' \\ y'' \\ z'' \end{pmatrix} = \begin{bmatrix} d_6 c_4 s_5 \\ d_6 s_5 s_4 \\ d_4 + d_6 c_5 \end{bmatrix} \qquad (181)$$

All the values in Eq.(181) are constants since the angles of joints 1 to 3 have already been found. From Eq. (181) the angles of the joints 4 and 5 are obtained:

$$\theta_4 = \tan^{-1}\left(\frac{y''}{x''}\right) + k\pi \tag{182}$$

$$\theta_5 = \tan^{-1}\left(\frac{y''}{s_4\left(z''-d_4\right)}\right) \tag{183}$$

When the angles of the first five joints are obtained, the position of the end effector is already determined. Joint six only changes the position of the end-effector.

Therefore the angle of the sixth joint is obtained from the desired orientation of the end effector:

$$A_6^0 = \begin{bmatrix} n_x & p_z & b_x & x \\ n_y & p_y & b_y & y \\ n_z & p_z & b_z & z \\ 0 & 0 & 0 & 1 \end{bmatrix} \tag{184}$$

$$n_6 = \begin{bmatrix} n_z \\ n_y \\ n_z \end{bmatrix} = \begin{bmatrix} \left[\left(c_1c_{23}c_4 + s_1s_4\right)c_5 - c_1s_{23}s_5\right]c_6 + \left(-c_1c_{23}s_4 + s_1c_4\right)s_6 \\ \left[\left(s_1c_{23}c_4 + c_1s_4\right)c_5 - s_1s_{23}s_5\right]c_6 + \left(-s_1c_{23}s_4 + c_1c_4\right)s_6 \\ \left(s_{23}c_4c_5 + c_{23}s_5\right)c_6 - s_{23}s_4s_6 \end{bmatrix} \tag{185}$$

To simplify the equations, the following variables are introduced:

$$\begin{aligned} \mu_1 &= \left[\left(c_1c_{23}c_4 + s_1s_4\right)c_5 - c_1s_{23}s_5\right] \\ \mu_2 &= \left(-c_1c_{23}s_4 + s_1c_4\right) \\ \mu_3 &= \left[\left(s_1c_{23}c_4 + c_1s_4\right)c_5 - s_1s_{23}s_5\right] \\ \mu_4 &= \left(-s_1c_{23}s_4 + c_1c_4\right) \\ \mu_5 &= \left(s_{23}c_4c_5 + c_{23}s_5\right) \\ \mu_6 &= -s_{23}s_4 \end{aligned}$$

From the angles of the joints 1 to 5 :

$$\begin{aligned} s_6 &= \frac{n_x\mu_3 - n_y\mu_1}{\mu_2\mu_3 - \mu_4\mu_1} \\ c_6 &= \frac{n_x\mu_4 - n_y\mu_2}{\mu_1\mu_4 - \mu_2\mu_3} \end{aligned} \tag{186}$$

Solving Eq.(186) gives:

$$\theta_6 = \tan^{-1}\left(\frac{s_6}{c_6}\right) + 2k\pi \tag{187}$$

The inverse kinematic equations contain many trigonometric terms which entail many possible solutions for any desired position of the end-effector.

Equation (173) has two solutions. Due to physical limitations, the angle of joint 1 needs to be between -10º a 90º.

Equations (176) and (177) that refer to angles θ_2 and θ_3 respectively have two possible solutions each. Knowing that joint 2 only can attain positive angles eliminates this ambiguity, allowing only solutions that give positive angles for these joints.

Equation (182), which gives the angle of joint 4, entails a singularity when the angle of joint 5 is zero. In this case the joints 4 and 6 are redundant. Joint 4 then has to be fixed in an arbitrary position. Joint 6 is then adjusted to give the desired orientation of the end-effector.

4.6. Orientation Error of the Manipulator

According to the model of generalized errors, the exact translation and orientation of the manipulator end-effector including errors is given by Eq.(10). When the manipulator structure has been calibrated, the end effector position can be estimated. However, the orientation of the end-effector cannot be estimated accurately since the rotary error $\varepsilon_{s,5}$ has been eliminated and transferred to the translational error $\varepsilon_{x,5}$. Also, the translational error $\varepsilon_{y,5}$ has been eliminated and transferred to the rotary error $\varepsilon_{p,5}$. This gives the right position, but the translation error of the end effector is not possible to estimate using the reduced set of errors. If the camera is placed on link 5 of the manipulator, it is the rotation error of link 5 that needs to be considered. The homogeneous matrix 4x4 that describes the orientation and position of the link 5 relative to its base as a function of the angles of the joints $\boldsymbol{\theta}=[\theta_1\ \theta_2\ \theta_3\ \theta_4\ \theta_5\ \theta_6]$ and the generalized errors $\boldsymbol{\varepsilon}$ is given by:

$$T_5^0(\theta,\varepsilon) = E_0 A_1^0 E_1 A_2^1 E_2 A_3^2 E_3 A_4^3 E_4 A_5^4 \tag{188}$$

This equation gives the actual position and orientation of link 5 given a full set of generalized errors. After the calibration of the robot, only the independent subset, $\boldsymbol{\varepsilon}^{\cdot}$ is available. This means that the eliminated errors of $\boldsymbol{\varepsilon}$ have to be substituted by zeros in the generalized error matrices. The deviation between the true and estimated orientation and position can then be given by:

$$\Delta T_5^0 = T_5^0(\theta,\varepsilon^{\cdot})^{-1} T_5^0(\theta,\varepsilon) = \begin{bmatrix} & & & \Delta X_5^0 \\ & \Delta R & & \Delta Y_5^0 \\ & & & \Delta Z_5^0 \\ 0 & 0 & 0 & 1 \end{bmatrix} \tag{189}$$

The nature of the deviation can be visualized in a simulation. By first defining a full 1 x 42 error vector and then estimating the reduced set of errors, the effects can be simulated.

$$\Delta R = \begin{bmatrix} \cos\Delta\theta_{y_5} & 0 & \sin\Delta\theta_{y_0} \\ 0 & 1 & 0 \\ -\sin\Delta\theta_{y_5} & 0 & \cos\Delta\theta_{y_0} \end{bmatrix} \cdot \begin{bmatrix} \cos\Delta\theta_{x_5} & -\sin\Delta\theta_{x_5} & 0 \\ \sin\Delta\theta_{x_5} & \cos\Delta\theta_{x_5} & 0 \\ 0 & 0 & 1 \end{bmatrix} \cdot \begin{bmatrix} 1 & 0 & 0 \\ 0 & \cos\Delta\theta_{z_5} & -\sin\Delta\theta_{z_5} \\ 0 & \sin\Delta\theta_{z_5} & \cos\Delta\theta_{z_5} \end{bmatrix} \quad (190)$$
$$= \begin{bmatrix} \Delta R_{11} & \Delta R_{12} & \Delta R_{13} \\ \Delta R_{21} & \Delta R_{22} & \Delta R_{23} \\ \Delta R_{31} & \Delta R_{32} & \Delta R_{33} \end{bmatrix}$$

The final expression for the relative rotation matrix will be:

$$\begin{bmatrix} \Delta R_{11} \\ \Delta R_{21} \\ \Delta R_{31} \end{bmatrix} = \begin{bmatrix} \cos\Delta\theta_{y_5}\cos\Delta\theta_{z_5} - \sin\Delta\theta_{x_5}\sin\Delta\theta_{y_5}\sin\Delta\theta_{z_5} \\ -\sin\Delta\theta_{z_5}\cos\Delta\theta_{x_5} \\ \sin\Delta\theta_{y_5}\cos\Delta\theta_{z_5} + \sin\Delta\theta_{x_5}\cos\Delta\theta_{y_5}\sin\Delta\theta_{z_5} \end{bmatrix}$$
$$\begin{bmatrix} \Delta R_{12} \\ \Delta R_{22} \\ \Delta R_{32} \end{bmatrix} = \begin{bmatrix} \cos\Delta\theta_{y_5}\sin\Delta\theta_{z_5} + \sin\Delta\theta_{x_5}\sin\Delta\theta_{y_5}\cos\Delta\theta_{z_5} \\ \cos\Delta\theta_{x_5}\cos\Delta\theta_{z_5} \\ \sin\Delta\theta_{x_5}\cos\Delta\theta_{z_5} - \sin\Delta\theta_{x_5}\cos\Delta\theta_{y_5}\cos\Delta\theta_{z_5} \end{bmatrix} \quad (191)$$
$$\begin{bmatrix} \Delta R_{13} \\ \Delta R_{23} \\ \Delta R_{33} \end{bmatrix} = \begin{bmatrix} -\sin\Delta\theta_{y_5}\cos\Delta\theta_{x_5} \\ \sin\Delta\theta_{x_5} \\ \cos\Delta\theta_{y_5}\cos\Delta\theta_{x_5} \end{bmatrix}$$

From Eq.(191) the relative rotation angles can be determined.

$$\Delta\theta_{y_5} = \tan^{-1}\left(-\frac{\Delta R_{13}}{\Delta R_{33}}\right) \quad (192)$$

$$\Delta\theta_{x_5} = \sin^{-1}\left(\Delta R_{2,3}\right) \quad (193)$$

$$\Delta\theta_{z_5} = \tan^{-1}\left(-\frac{\Delta R_{21}}{\Delta R_{22}}\right) \quad (194)$$

To get an idea of the magnitude of the orientation errors of link 5 there a simulation was performed. The actual generalized position errors were chosen randomly in the interval +/- 2 mm and the rotational errors in the interval +/- 1° = +/- π/180 radians. 100 measurements of the end-effector were simulated and the reduced error vector, $\boldsymbol{\varepsilon}$, was estimated.

Error	$\boldsymbol{\varepsilon}$	Actual $\dot{\boldsymbol{\varepsilon}}$	Estimated $\dot{\boldsymbol{\varepsilon}}$
$\varepsilon_{x,0}$	$-4{,}37216\cdot10^{-1}$	$-4{,}37216\cdot10^{-1}$	$-4{,}37216\cdot10^{-1}$
$\varepsilon_{y,0}$	$-7{,}13467\cdot10^{-1}$	$-7{,}13467\cdot10^{-1}$	$-7{,}13467\cdot10^{-1}$
$\varepsilon_{z,0}$	$1{,}36214\cdot10^{0}$	0	0
$\varepsilon_{s,0}$	$-7{,}72363\cdot10^{-3}$	$-7{,}72363\cdot10^{-3}$	$-7{,}72363\cdot10^{-3}$
$\varepsilon_{r,0}$	$-7{,}85205\cdot10^{-3}$	0	0
$\varepsilon_{p,0}$	$-4{,}78854\cdot10^{-3}$	$-4{,}78854\cdot10^{-3}$	$-4{,}78854\cdot10^{-3}$
$\varepsilon_{x,1}$	$-1{,}37638\cdot10^{0}$	$-1{,}37638\cdot10^{0}$	$-1{,}37638\cdot10^{0}$
$\varepsilon_{y,1}$	$1{,}10429\cdot10^{0}$	$2{,}46643\cdot10^{0}$	$2{,}46643\cdot10^{0}$
$\varepsilon_{z,1}$	$-1{,}68456\cdot10^{0}$	0	0
$\varepsilon_{s,1}$	$-1{,}12305\cdot10^{-3}$	$-8{,}97510\cdot10^{-3}$	$-8{,}97510\cdot10^{-3}$
$\varepsilon_{r,1}$	$-3{,}92045\cdot10^{-3}$	0	0
$\varepsilon_{p,1}$	$1{,}44530\cdot10^{-2}$	$1{,}44530\cdot10^{-2}$	$1{,}44530\cdot10^{-2}$
$\varepsilon_{x,2}$	$1{,}90693\cdot10^{-1}$	$1{,}90693\cdot10^{-1}$	$1{,}90693\cdot10^{-1}$
$\varepsilon_{y,2}$	$1{,}04412\cdot10^{0}$	$-1{,}90798\cdot10^{0}$	$-1{,}90798\cdot10^{0}$
$\varepsilon_{z,2}$	$-1{,}87452\cdot10^{0}$	0	0
$\varepsilon_{s,2}$	$-1{,}34867\cdot10^{-2}$	$-1{,}34867\cdot10^{-2}$	$-1{,}34867\cdot10^{-2}$
$\varepsilon_{r,2}$	$-2{,}85224\cdot10^{-3}$	0	0
$\varepsilon_{p,2}$	$6{,}75503\cdot10^{-3}$	$6{,}75503\cdot10^{-3}$	$6{,}75503\cdot10^{-3}$
$\varepsilon_{x,3}$	$1{,}01659\cdot10^{0}$	$1{,}01659\cdot10^{0}$	$1{,}01659\cdot10^{0}$
$\varepsilon_{y,3}$	$1{,}73229\cdot10^{0}$	$-9{,}23807\cdot10^{-1}$	$-9{,}23807\cdot10^{-1}$
$\varepsilon_{z,3}$	$-2{,}53265\cdot10^{-1}$	0	0
$\varepsilon_{s,3}$	$3{,}02161\cdot10^{-3}$	$-3{,}75109\cdot10^{-3}$	$-3{,}75109\cdot10^{-3}$
$\varepsilon_{r,3}$	$-2{,}77296\cdot10^{-3}$	0	0
$\varepsilon_{p,3}$	$3{,}33908\cdot10^{-3}$	$3{,}33908\cdot10^{-3}$	$3{,}33908\cdot10^{-3}$
$\varepsilon_{x,4}$	$-1{,}72555\cdot10^{0}$	$-1{,}72555\cdot10^{0}$	$-1{,}72555\cdot10^{0}$
$\varepsilon_{y,4}$	$1{,}82347\cdot10^{0}$	$8{,}03470\cdot10^{-1}$	$8{,}03470\cdot10^{-1}$
$\varepsilon_{z,4}$	$1{,}89196\cdot10^{0}$	0	0
$\varepsilon_{s,4}$	$2{,}72558\cdot10^{-3}$	$5{,}49854\cdot10^{-3}$	$5{,}49854\cdot10^{-3}$
$\varepsilon_{r,4}$	$1{,}35406\cdot10^{-2}$	0	0
$\varepsilon_{p,4}$	$9{,}10026\cdot10^{-3}$	$9{,}10026\cdot10^{-3}$	$9{,}10026\cdot10^{-3}$
$\varepsilon_{x,5}$	$-1{,}09157\cdot10^{0}$	$9{,}30879\cdot10^{0}$	$9{,}30879\cdot10^{0}$
$\varepsilon_{y,5}$	$1{,}99076\cdot10^{0}$	0	0
$\varepsilon_{z,5}$	$2{,}49776\cdot10^{-1}$	0	0
$\varepsilon_{s,5}$	$1{,}53493\cdot10^{-2}$	0	0
$\varepsilon_{r,5}$	$-4{,}35010\cdot10^{-3}$	0	0
$\varepsilon_{p,5}$	$-4{,}28421\cdot10^{-3}$	0	0
$\varepsilon_{x,6}$	0	0	$-4{,}00000\cdot10^{-15}$
$\varepsilon_{y,6}$	0	0	$-5{,}00000\cdot10^{-15}$
$\varepsilon_{z,6}$	0	$2{,}49776\cdot10^{-1}$	$2{,}49776\cdot10^{-1}$
$\varepsilon_{s,6}$	0	0	0
$\varepsilon_{r,6}$	0	0	0
$\varepsilon_{p,6}$	0	0	0

Table 2 – Errors from simulation

Table 2 shows the errors that were used in the simulation. The difference between the actual $\dot{\boldsymbol{\varepsilon}}$ and the estimated $\dot{\boldsymbol{\varepsilon}}$ was less than 10^{-12} for all elements of $\dot{\boldsymbol{\varepsilon}}$.

The actual manipulator was not used in this experiment, so the results only demonstrate the accuracy of the manipulator given that the nonrepetitive errors of the manipulator are neglectable.

The magnitude of the rotation error, ΔR was then estimated for 100 different configurations of the joints. The configurations of the six joints were chosen randomly within the possible movement for each joint. The rotation and position errors for link 5 and the end-effector are then plotted. Figure 36 shows the position error of the end-effector for the different configurations. The graph shows that the position error is negligible for such a big manipulator.

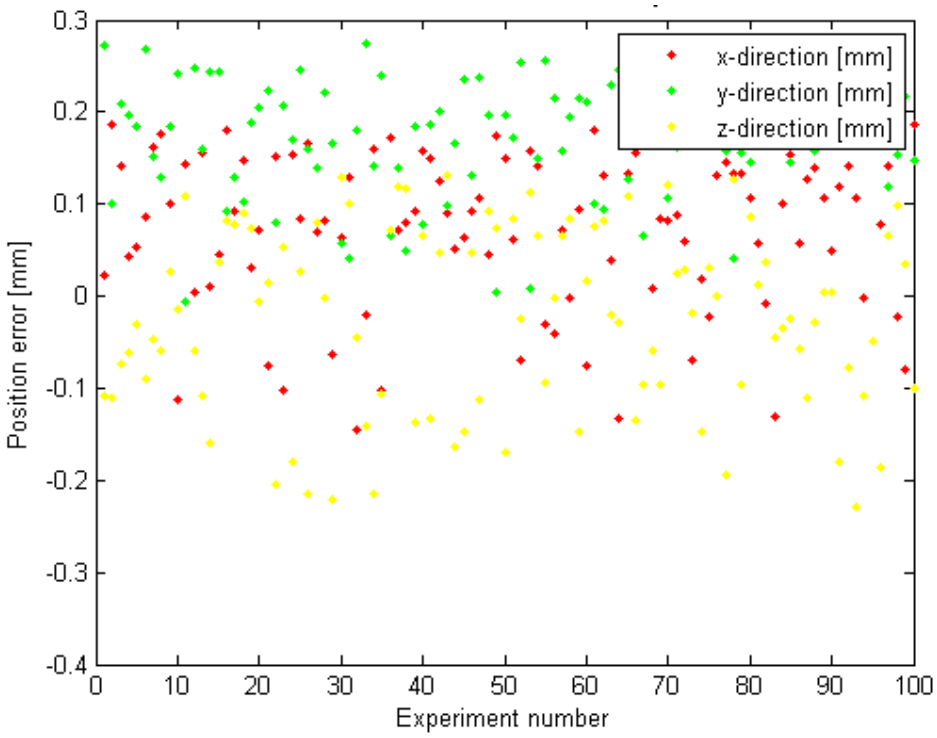

Figure 36 - Position error of end-effector after calibration

Figure 37 shows the rotation error of the end-effector after calibration. It is obvious that the rotation error of the end-effector is too big to be used as base for the camera.

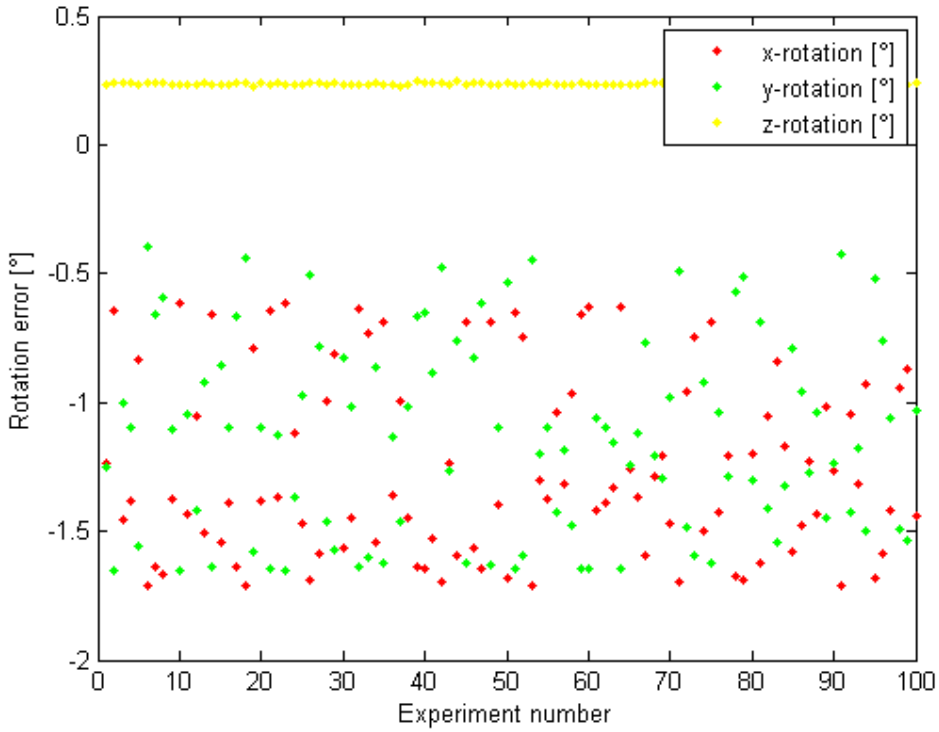

Figure 37 - Rotation error at the end effector after calibration

Figure 38 shows the position error of link 5. The position error is almost constant. This means that a camera that is attached link 5 will have a fixed deviation from its estimated position. This deviation can be found through calibration.

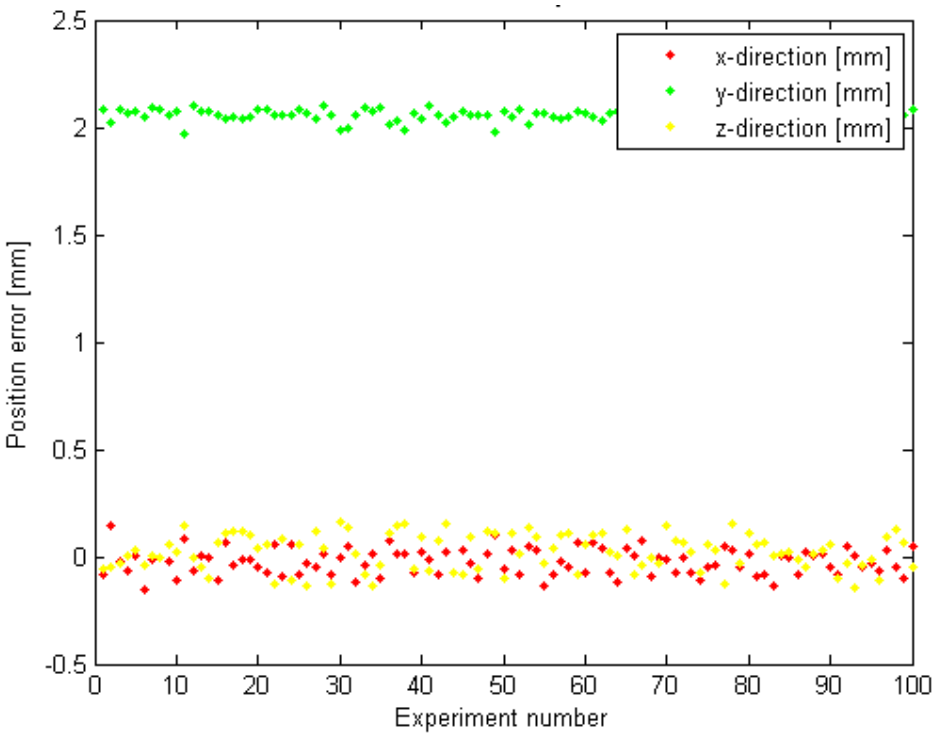

Figure 38 - Position error of link 5 after calibration

Figure 39 shows the rotation error of link 5. Also the rotation error is constant. The rotation error around the y axis is large compared to the other rotation errors. From table 2, it can be seen that the error $\varepsilon'_{x,5}$ is badly estimated. According to Eq.(167) this error is connected with the rotation error around the y axis of joint 5, $\varepsilon'_{s,5}$. Since the contribution on the end-effector position from these two errors cannot be distinguished, the rotation error around the y axis is large when , $\varepsilon'_{x,5}$ is large.

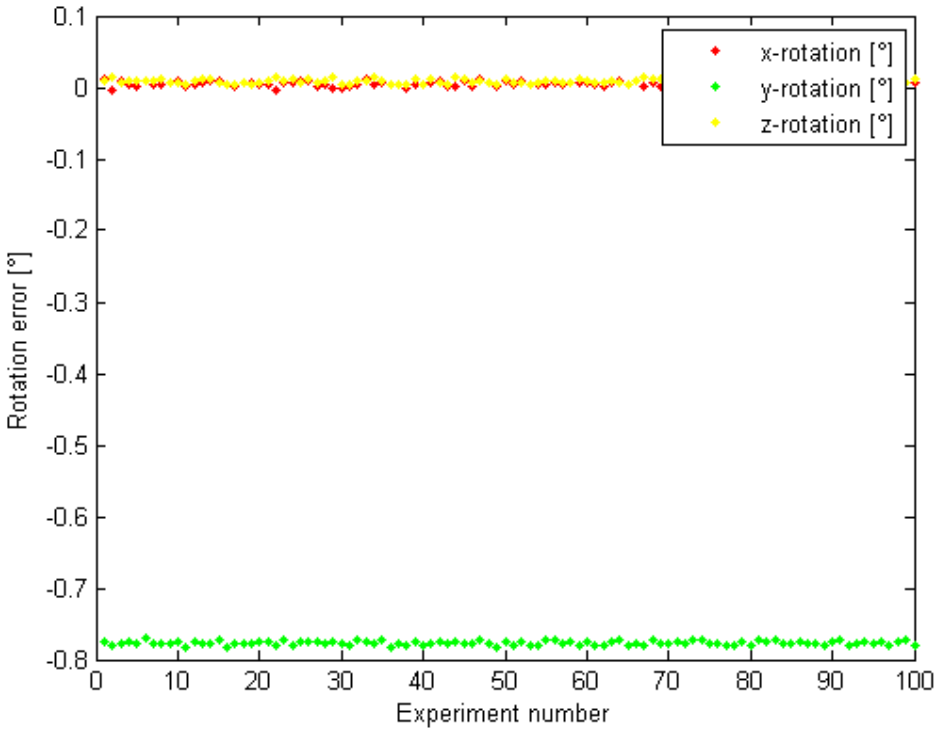

Figure 39 - Rotation error of link 5 after calibration

After estimating all error parameter, the kinematic model of the manipulator can be used to calibrate the robot base using the vision techniques previously described. Experimental results are presented next.